Biophysical Chemistry 12 (1980) 307–315

KINETICS OF THE COOPERATIVE ASSOCIATION OF T4 TAIL SHEATH PROTEIN P18 TO POLYSHEATHS

Jürg TSCHOPP and Jürgen ENGEL
Dept. of Biophysical Chemistry, Biozentrum Universität Basel, Switzerland

Received 20 May 1980

The polymerization of the monomeric sheath protein P18 to polysheath was followed by light scattering in 1 mM sodium phosphate buffer, pH 7 at a $MgCl_2$ concentration of 5 mM. Sigmoidal kinetics were observed in the case of spontaneous nucleation. These were well fitted by a mechanism involving a slow nucleation step (rate constant $k_N = 10^{-2}\ M^{-1}\ s^{-1}$) followed by propagation steps ($k = 10^5\ M^{-1}\ s^{-1}$) in which P18 protomers are added to the ends of the polysheath particles. When sonicated polysheats or contracted sheaths were added as seeds exponential time courses were observed. From the pseudo first order rate constant and the concentration of seeds the above value for the rate constant of propagation was confirmed. The ability of contracted sheaths to nucleate polysheath formation lends support to the conclusion that polysheaths and contracted sheaths have identical structures and differ in their length distributions only. These were measured from electromicrographs and from the distribution of sedimentation coefficients. Poisson type, kinetically controlled size distributions were found after polymerization of polysheath. An extremely slow redistribution towards an exponential distribution was detected. The spontaneous slow formation of polysheaths is much slower than the formation of extended sheath at core baseplates. Extended sheath is a metastable assembly product of P18 which either dissociates or contracts to form contracted sheath. Polysheaths and contracted sheaths are extremely stable products but their immediate formation is hindered by high nucleation difficulties.

1. Introduction

The T4 tail is a complex structure requiring at least 21 gene products for its assembly. It consists of a hexagonal baseplate on which a core of 144 protomers (gene product P19) is attached. The core is surrounded by the same number of protomers P18 forming the sheath. Gene products P15 and probably P3 bind to the end of the core sheath complex at which the head is attached later in the assembly process [1].

The sheath is a metastable organelle. During infection the extended sheath contracts to form the contracted sheath [2]. Both structures have been well characterized by three-dimensional image processing [3,4]. The extended sheath consists of 24 annuli each with 6 protomers of P18. The distance between two annuli is 4.11 nm. A rearrangement is observed during contraction by which the overall length is reduced from about 95 nm to 38 nm.

The assembly pathway of the tail starts with the formation of the baseplate which nucleates core formation. P18 assembles to the core-baseplates [5,6]. Mutants, in which the formation of core-baseplate is blocked, produce polysheaths, an aberrant polymerization product of P18. Optical diffraction patterns of polysheaths [7] show a striking similarity with those of contracted sheath. Polysheaths occur in much longer length than contracted sheaths. Although the general arrangement of P18 in both structures seems to be identical polysheaths seem to be more flexible and appears to have a somewhat irregular surface [8].

Recently an isolation procedure of monomeric P18 was described [9]. This offered the possibility to polymerize P18 into polysheaths *in vitro* and to study the kinetics of its assembly. The present study was undertaken in view of the competition of polysheath formation with the assembly of the extended sheath [6]. It was shown that seeds of contracted sheath can nucleate polysheath formation. This is a sensitive test for the relatedness of the two structures.

2. Materials and methods

2.1. P18 and contracted sheath isolation

P18 was isolated from T4 tails according to Tschopp et al. [9]. Isolation of contracted sheaths was carried out by trypsin treatment of T4 phage [10] or by treatment with potassium hydroxide, pH 12.9 [11].

2.2. Protein concentration

The concentration of monomeric P18 was determined spectrophotometrically using an extinction coefficient of $E = 890\ \mathrm{cm^2\ g^{-1}}$ [9]. The concentration of contracted sheath was determined according to Lowry et al. [12] with bovine serum albumin as a standard. Molar concentrations were calculated with the molecular weight of 65000 of P18 [9].

2.3. Polymerization followed by light scattering

Light scattering measurements were carried out in a Farrand spectrofluorimeter Mark I. Excitation and emission wavelength were set at $\lambda = 436$ nm and the intensity of light-scattering was monitored at an observation angle of 90°. Stock solutions of P18 were centrifuged at 250000 g for 40 minutes to remove dust and polymers prior to use. The temperature in the cell was 20° ± 0.2°C. Polymerization of P18 in 1 mM sodium phosphate buffer, pH 7 was initiated by rapid addition of 0.1 ml $MgCl_2$ dissolved in the same buffer to a final concentration of 5 mM. When contracted sheaths or sonicated polysheaths were used as nuclei, they were dissolved in 2 ml 1 mM sodium phosphate buffer, pH 7 containing 6.25 mM $MgCl_2$ and mixed with 0.5 ml P18 solution in the same buffer without $MgCl_2$.

2.4. Electron microscopy

Samples were applied to carbon coated grids rendered hydrophylic by glow discharge and negatively stained with 2% phosphotungstic acid, pH 7.2. They were examined in a Philips EM 300 electron microscope. For length determinations several hundred polymers from different mesh fields and grids were measured.

2.5. Ultracentrifugation

Sedimentation velocities were measured in a Beckman Spinco Model E analytical ultracentrifuge equipped with scanner at an angular velocity of $\omega = 2094.4$ radian · s^{-1} and 20°. The normalized sedimentation distribution function [13,14]

$$g(s) = \frac{1}{C_0}\frac{dC_0}{ds} = \frac{1}{C_0}\frac{dC_0}{dx}\frac{dx}{ds} = \frac{1}{C_0}\frac{dC}{dx}\left(\frac{x}{x_m}\right)^2 x\omega^2 t \quad (1)$$

was evaluated from the sedimentation profile neglecting the effect of diffusion. This is possible for very large particles with very small diffusion coefficients [14]. C is the weight concentration at position x from the rotor centre, C_0 is the initial concentration in the plateau region and s is the sedimentation coefficient. The factor x^2/x_m^2 in which x_m is the position of the meniscus corrects for radial dilution [13]. The "true" sedimentation time t was evalutated from a plot log $x_{0.5}$ versus time [14] where $x_{0.5}$ is the position of the midpoint of the boundary. It is the interval between the time at which the straight line of this plot intersects x_m and the time at which the sedimentation profile was recorded.

3. Results

3.1. Evalutation of P18 incorporation into polysheath by light scattering

The formation of polysheath was monitored by the changes of light scattering intensity $R(\theta)$ at an observation angle θ and a wavelength $\lambda = 436$ nm. It was shown [15] that for long rod-like particles with length

$$L \gg \lambda^* = \lambda(4\pi \sin\theta/2)^{-1}, \quad (2)$$

$$R(\theta) = A c_p^* \lambda^*, \quad (3)$$

where $c_p^* = c_A^0 - c_A$ is the molar concentration of protomers incorporated into the rod-like particles; c_A^0 is the total protomer concentration and c_A is the concentration of free monomers. A is a constant [15] for a given system and experimental set-up. It was determined from the end value of $R(\theta)$ observed after complete polymerization ($c_p^* \approx c_1^0$).

Eq. (3) predicts a linear dependence of $1/R(\theta)$ on $\sin(\theta/2)$. Such a dependence was indeed observed

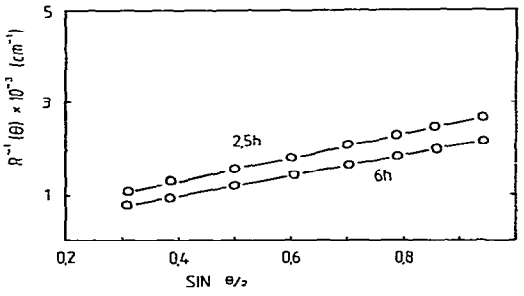

Fig. 1 Angular dependence of light scattering intensity. Polysheaths were formed by spontaneous nucleation at a total concentration of P18 of c_A^0 = 1.14 μM in 1 mM sodium phosphate buffer, pH 7 containing 5 mM $MgCl_2$ during 2.5 and 6 h respectively. The reciprocal light scattering intensity R^{-1} is plotted versus sin (θ/2) according to eqs. (2) and (3), where θ is the observation angle relative to the incident beam. The wavelength was λ = 436 nm and the temperature was 20°C.

(fig. 1) and proves the applicability of eq. (3). The value of λ^* is 37 nm for λ = 436 nm and an observation angle of 90°. The polysheaths which were observed electronmicroscopically (see section 3.4) were much longer than 37 nm. Another test for $L > \lambda^*$ is the independence of light scattering intensity on the length of the polysheath. When the electronmicroscopically observed average length was reduced from 232 nm to 119 nm by sonication $R(90°)$ decreased by only 4%. Eq. (3) is not applicable for the very initial phase of polymerization when L is till smaller than λ^*. It is however considered to be a good approximation for the experimentally observed initial phase because of the high cooperativity of polysheath formation. This leads to an immediate formation of long filaments. The light scattering intensity due to P18 monomers present in solution is extremely small as compared with the scattering of the polysheaths and was neglected.

3.2. Kinetics of polysheath formation with spontaneous nucleation

Polysheath formation was initiated by addition of Mg^{2+} (final concentration 5 mM) to solutions of monomeric P18 in 1 mM sodium phosphate buffer, pH 7. The time course of polymerization was monitored by the increase of light scattering intensity from which the concentration of protomers incorporated into polysheath c_p^* was calculated with eq. (3). This

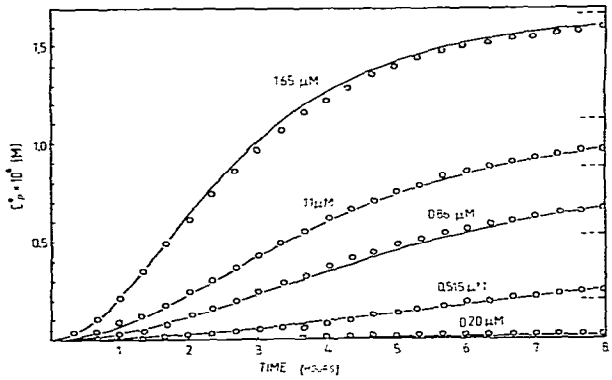

Fig. 2. Spontaneous polymerization of P18 to polysheath followed by light scattering. Polymerization was induced by addition of $MgCl_2$ (final concentration 5 mM) to solutions of P18 in 1 mM sodium phosphate buffer, pH 7 at 20°C. Total P18 concentrations c_A^0 are indicated. The molar concentration of P18 protomers incorporated into polysheath c_p^* was calculated by eq. (3) from the observed changes in light scattering intensity (○). End values measured after 2 to 4 days are represented by dotted lines. The curves were calculated for mechanism (4) and (5) by numerical integration of eqs. (6) and (7) with x = 2 and $k\,k_N$ = 8000 $M^{-2}\,s^{-2}$.

quantity is plotted as a function of time for various total concentrations of P18 (fig. 2). The curves are sigmoidal and highly concentration dependent. At the highest concentration a plateau value of light scattering intensity at $c_p^* = c_A^0$ was reached after 10 h. In all experiments final values were measured after 2 to 4 days. Reversibility was examined by addition of 5 mM EDTA after polymerization. EDTA chelates Mg^{2+} and reduces its concentration to a level at which no polymerization takes place [9]. After addition of EDTA the light scattering intensity did not decrease. It was also not possible to dissociate polysheath by dialysis against plain buffer without Mg^{2+} for a period of several days. Irreversibility can therefore be assumed on the time scale of the polymerization experiments. The length distribution of the polysheaths changes at a much larger time scale as will be shown in section 3.4.

The results exhibit the distinctive features of an irreversible polymerization in which a spontaneous slow nucleation of polysheath is followed by faster elongation steps [15,16]. For a simple quantitative description we assume that x protomers form a nucleus A_x with a rate constant k_N

$$x\,A \xrightarrow{k_N} A_x. \qquad (4)$$

It is reasonable to assume that the reaction steps in which further protomers are associated to the ends of a nucleus or to longer polysheaths are essentially equal and proceed with a rate constant k

$$A_i + A \xrightarrow{k} A_{i+1}, \quad x \leqslant i < n. \tag{5}$$

The concentration of polysheath filaments c_p increases according to

$$dc_p/dt = k_N c_A^x. \tag{6}$$

The rate of protomer incorporation into the growing polysheath is

$$dc_p^*/dt = k c_A c_p = k c_p (c_A^0 - c_p^*). \tag{7}$$

Numerical integration of eqs. (6) and (7) yielded an excellent fit of the experimentally observed time courses and their concentration dependence with $x=2$ and $k k_N = 8000\ M^{-2}\ s^{-2}$.

It is not possible to determine k and k_N separately [15] from the time dependence of c_p^* alone. It is however possible to estimate k and k_N from a determination of the concentration of polysheaths $c_p(\vartheta)$ at time ϑ after the start of polymerization. With the integrated form of eq. (6) for $x=2$ it follows

$$k_N = c_p(\vartheta) \Big/ \int_0^{\vartheta} (c_A^0 - c_p^*)^2\, dt. \tag{8}$$

The polymerization kinetics was followed at a total P18 concentration of $c_A^0 = 3.3\ \mu M$ by light scattering and a c_p^* versus time curve similar to those shown in fig. 2 was recorded. At time $\vartheta = 12$ h a sample was inspected electronmicroscopically. Polymerization was essentially complete and the size distribution of the polysheath did not change during the time needed to prepare the electronmicroscopic specimen. The average length of the polysheaths was 232 nm. With the pitch of 0.266 nm per protomer in the polysheath structure [3,4] an average number of protomers of $\langle n \rangle = 870$ per particle was calculated. The concentration of polysheath particles was therefore $c_p(\vartheta = 12\ h) = c_p^*/\langle n \rangle \approx c_A^0/\langle n \rangle = 3.8$ nM. The integral in eq. (8) was determined by numerical integration of the c_p^* versus time curve and a value of $k_N = 9 \times 10^{-2}\ M^{-1}\ s^{-1}$ was obtained. From this value and the known value of the product $k_N k = 8000\ M^{-2}\ s^{-2}$ the rate constant of elongation k is estimated to be $9 \times 10^4\ M^{-1}\ s^{-1}$.

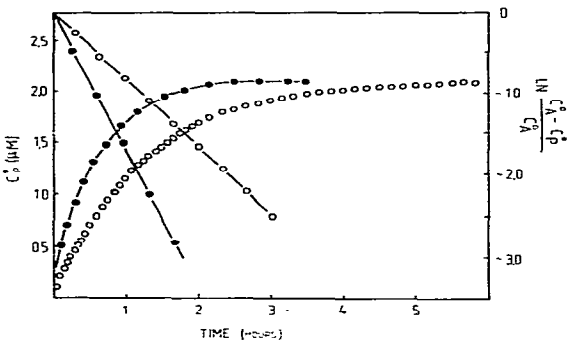

Fig. 3. Seeded polymerization of P18 to polysheath followed by light scattering. Polymerization was initiated by addition of seeds of sonicated polysheath (—○—) or contracted sheath (—●—). The total P18 concentration was $c_A^0 = 2.11\ \mu M$. All other conditions were as described in the legend of fig. 2. The concentration of sonicated polysheath particles was $c_p = 3.77$ nM. A pseudo first order rate constant $k_{obs} = 2.16 \times 10^{-4}\ s^{-1}$ was obtained from a first order plot (left ordinate). When contracted sheaths were used as seeds c_p was 17 nM and $k_{obs} = 4.46 \times 10^{-4}\ s^{-1}$ was obtained.

3.3. Seeded polysheath formation

When polymerization was initiated by simultaneous addition of $MgCl_2$ and nuclei to a solution of monomeric P18 first order kinetics was observed for the increase of c_p^* with time (fig. 3). In this case the necessity for spontaneous slow nucleation is eliminated and the polymerization process proceeds by elongation of the added nuclei according to eq. (7). The concentration of nuclei is constant and equal to c_p. Pseudo first order rate constants $k_{obs} = k c_p$ are therefore obtained from first order plots of the polymerization kinetics (fig. 3).

Two types of seeds, sonicated polysheath and contracted sheath were used. Polysheath $c_p^* = 1.68\ \mu M$ was sonicated for 2 min. The average length of the filaments as determined from electronmicrographs (section 3.4) decreased from 232 nm to 119 nm (corresponding to an average length of $\langle n \rangle = 445$). The concentration of seeds was $c_p = c_p^*/\langle n \rangle = 3.77$ nM. From $k_{obs} = k c_p = 2.1 \times 10^{-4}\ s^{-1}$ (fig. 3) a value of $k = 5.8 \times 10^4\ M^{-1}\ s^{-1}$ was calculated which is in good agreement with the value obtained from the analysis of the kinetics with spontaneous nucleation.

When contracted sheaths were used as seed $c_p =$

Table 1
Rate constant of polysheaths nucleation (k_N) and elongation (k)

	k_N (M^{-1} s^{-1})	k (M^{-1} s^{-1})
spontaneous nucleation	$(9 \pm 5) \times 10^{-2}$	$(9 \pm 3) \times 10^4$
polymerization seeded with sonificated polysheaths	–	$(7 \pm 3) \times 10^4$
contracted sheaths	–	$(4 \pm 3) \times 10^4$

Error limits were estimated from two to four kinetic experiments and from the error limits of the determination of c_A^0 and c_p.

17 nM was calculated from the weight concentration and the known number of protomers $n = 144$ [1] in the contracted sheath. Again first order kinetics was observed and a value of $k = 6.2 \times 10^4$ M^{-1} s^{-1} was obtained from the pseudo first order rate constant $k_{obs} = 4.46 \times 10^{-4}$ s^{-1}.

The rate constants which were obtained from these and similar experiments are summarized in table 1.

3.4. Electromicrographs and length distributions

Polysheaths which were formed by spontaneous nucleation were inspected by electronmicroscopy. They exhibited the normal appearance [3,8] resembling that of contracted sheath but with some irregularities and gaps in the surface. The length distribution of a preparation which was polymerized at a total P18 concentration of $c_A^0 = 3.3$ μM for a period of 12 h is shown in fig. 4. The average length was $\langle n \rangle = 232$ nm.

When the sample was sonicated for 2 min the average length decreased to 119 nm and a more exponential length distribution was observed (fig. 5). This sample was used for the experiments in which polysheath was used as seeds for polymerization.

When polysheath formation was seeded by contracted sheath electronmicrographs revealed that P18 indeed associated onto the contracted sheath particles (fig. 6). However in many instances the contracted sheaths with their length of 36 nm were still distinguishable as parts of the particles formed. Particularly at the end of newly formed polysheath a region of this length with a more regular structure than that of polysheath was seen (fig. 6). Also gaps with high stain penetration were often seen between the seeds and the newly formed structures. When the samples

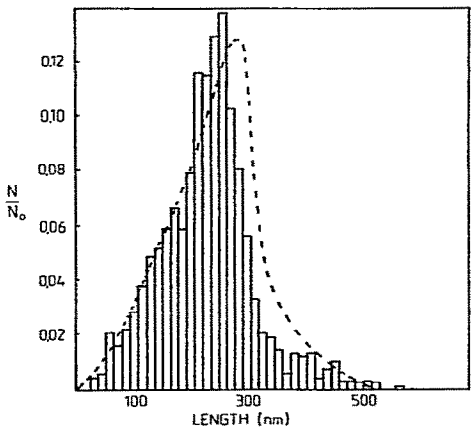

Fig. 4. Length distribution of polysheths observed in electronmicrographs and derived from the distribution of sedimentation coefficients. Polysheaths were formed by spontaneous nucleation at at total P18 concentration of $c_A^0 = 3.3$ μM for 12 h (for other conditions see legend of fig. 2). The length of a total of $N_0 = 438$ particles was measured in electronmicrographs. The columns represent the fraction of particles N/N_0 with a length ($L \pm 7$) nm. For the same sample the size distribution was determined from the distribution of sedimentation coefficients. The corresponding curve was calculated by eq. (1) as described in the text.

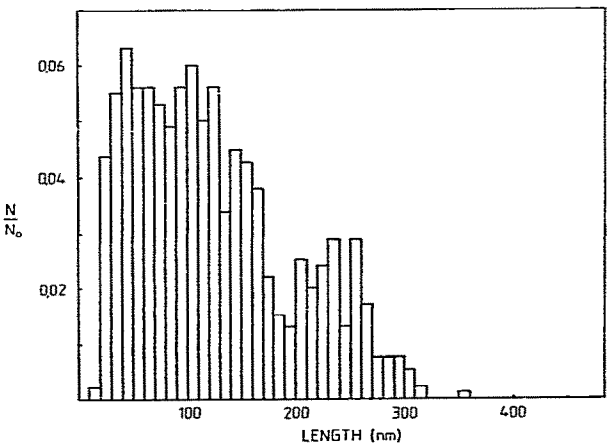

Fig. 5. Length distribution of sonicated polysheaths observed by electronmicroscopy. The sample whose length distribution is shown in fig. 4 was sonicated for 2 min and inspected by the electronmicroscope immediately. The length of 411 particles was measured.

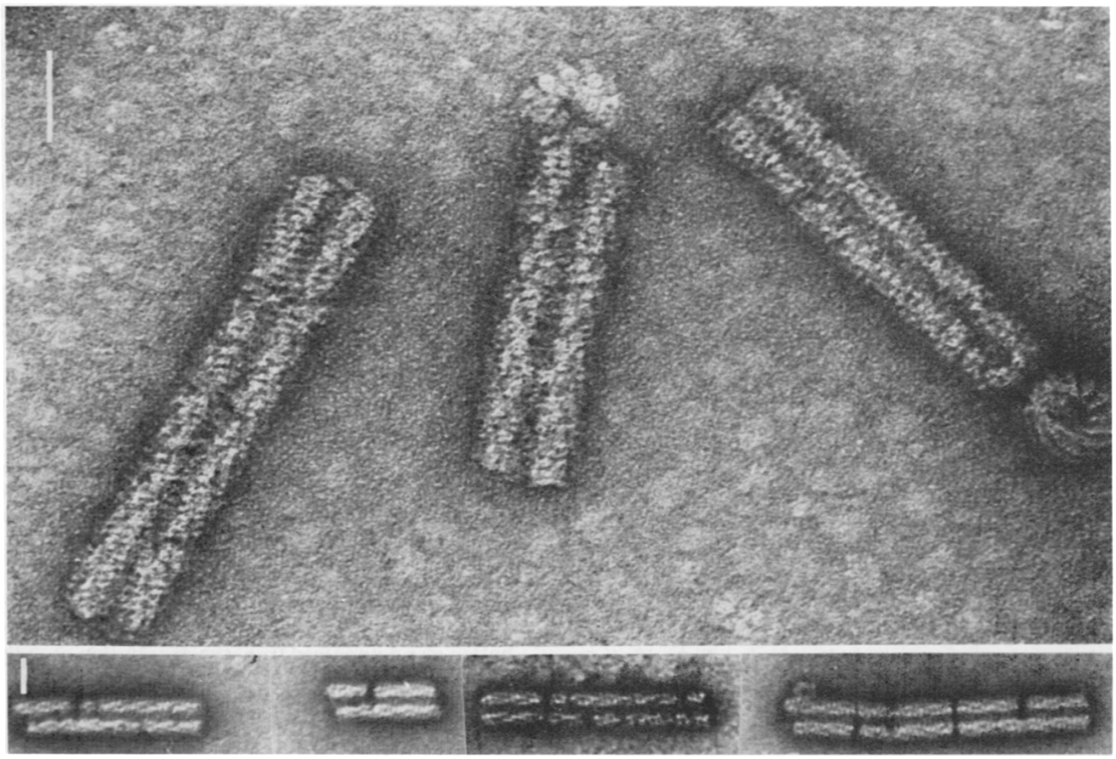

Fig. 6. Electronmicrographs of polysheaths formed by nucleation with contracted sheath. Polymerization of P18 total concentration c_A^0 = 2.11 μM was nucleated with seeds of contracted sheath (c_p = 3.77 nM) in 1 mM sodium phosphate buffer, pH 7 containing 5 mM $MgCl_2$ at 20°C and inspected electronmicroscopically after 12 h. The white bars correspond to a length of 30 nm.

were inspected again after several weeks these features had largely disappeared and all parts of the particles exhibited a more regular appearance. Also the morphological irregularities normally observed in polysheath disappeared with time when samples were kept at 4°C for several weeks.

3.5. Length distributions from the distribution of sedimentation coefficients

The sedimentation profile was recorded for the same sample of spontaneously nucleated polysheath for which the length distribution was determined by electronmicroscopy (see section 3.4) and the sedimentation distribution function $g(s)$ was determined by eq. (1). In order to determine the length distribution the dependence of the sedimentation coefficients s on length has to be known. This function was derived [17] for cylindrical particles of length L, diameter d and molecular weight per length ratio γ

$$s = \gamma \frac{(1-\upsilon_2\rho)}{6\pi\eta N_A}\left(2\ln\frac{2L}{d} + \frac{d}{L} - 0.2316\right). \qquad (9)$$

N_A is Avogadro's number, η and ρ the viscosity and density of the solvent respectively and υ_2 is the partial specific volume of the solute. For polysheath, d = 25 nm and γ = 24600 nm^{-1}.

With the known function $g(s)$ the weight fraction of molecules $\delta C_0/C_0 = g(s)\,\delta s$ with a sedimentation coefficient s was calculated. Sedimentation coefficients were transformed to lengths L by means of eq. (9). The fraction of particles $\delta N/N_0$ with length L was cal-

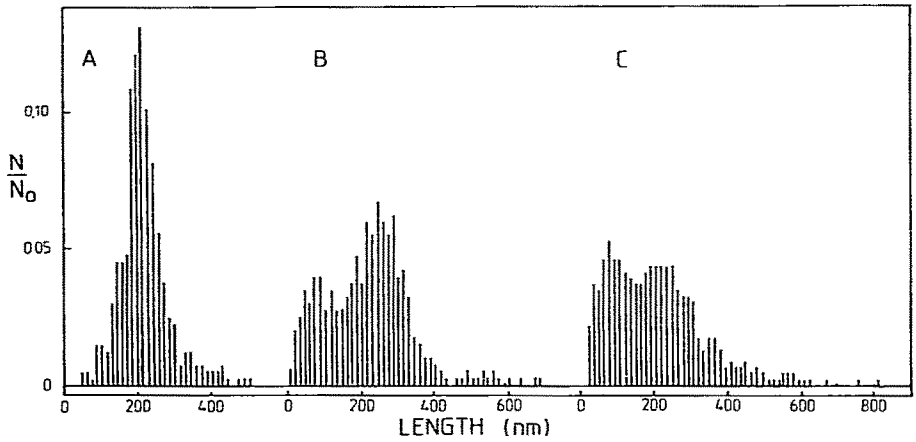

Fig. 7. Change of the length distribution of polysheath with time. Polysheath was formed as described in the legend of fig. 4. Samples were kept at 4°C and the size distribution was measured electronmicroscopically after 4 days (A), 35 days (B) and 85 days (C).

culated by devision of $\delta C_0/C_0$ by L and by a normalization factor. The latter was determined from the condition that the integral over $\delta N/N_0$ must be equal to 1. The resulting length distribution is compared in fig. 4 with the length distribution which was measured electronmicroscopically for the same sample. A satisfactory agreement is observed between the results of the two methods.

3.6. Change of the length distribution with time

A slow redistribution of the initially formed kinetically controlled Poisson type distribution of particle lengths is expected on theoretical grounds [16,18]. For polysheaths which were formed by spontaneous polymerization at a total P18 concentration of c_A^0 = 3 μM at 20° C size distribution similar to that shown in fig. 4 was observed after 12 h. No significant changes were detectable during 4 days. When the sample was kept for very long periods of time (fig. 7) a broadening and changes towards a more exponential type of distribution were observed. The experiments were performed at 4° in order to prevent bacterial growth. The rates of changes are therefore not directly comparable with the rate of polymerization at 20°C.

4. Discussion

Polysheath was first detected as an aberrant polymerization product in lysates of E. coli bacteria infected with T4 mutants in which the formation of core baseplates was blocked [19,20]. The present data demonstrate that polysheaths are formed by spontaneous but slow nucleation from purified P18 monomers in the presence of Mg^{2+} or other cations. The polymerization kinetics is well described by a mechanism which consists of an irreversible nucleation step leading to a dimer of two P18 protomers followed by irreversible and faster elongation steps which all proceed with the identical rate constants. Under the conditions used for the kinetic studies (5 mM Mg^{2+}, 20°C) nucleation was 10^6 times slower than elongation. A value of 9×10^4 M^{-1} s^{-1} was obtained for the rate constant of elongation from an analysis of the sigmoidal time course observed for spontaneous nucleation. Very similar values followed from the first order kinetics when the nucleation difficulty was eliminated by addition of seeds. This good agreement proves the applicability of the reaction mechanism assumed for the spontaneous nucleation. The rate constant of elongation is several orders of magnitude slower than diffusion controlled. By analogy with the well studied interaction of pancreatic trypsin inhibitor with trypsin or α-chymotrypsin [21,22] it is likely

that each elongation step implies a diffusion controlled encounter followed by a rate determining monomolecular conformational change or rearrangement of the newly added P18 protomer. The elongation of polysheath is somewhat faster than the elongation of actin filaments [15].

Extended sheath is another assembly form of P18 which is stabilized by interactions with the core baseplate and possibly with gene products P3 and P15 located at the end of the core [1]. No conditions are known at which extended sheath is formed in the absence of core baseplates. When core baseplates are present as nuclei the formation of extended sheath is much faster [6] than the slow spontaneous formation of polysheath. Extended sheath is therefore a metastable structure which is readily transformed to contracted sheath by the attachment of T4 phage to the surface of the host cells [8] but also by a number unphysiological trigger mechanisms [8]. Contracted sheath is extremely stable and is the only phage organelle which withstands treatment with 8 M urea [8].

Image reconstruction studies [3,4] revealed a close resemblance of the structures of contracted sheath and polysheath. The present finding that contracted sheath can nucleate polysheath polymerization equally well as seeds of polysheath is a strong additional proof for the identity of the two structures. The often observed irregularities in the surface of polysheath as contrasted to contracted sheath are explained by the different pathways of formation. When the core baseplate serves as a matrix for extended sheath formation a very regular arrangement of P18 protomers is obtained. During contraction large changes of the arrangement occur but the regularity is preserved. During spontaneous polymerization without a matrix assembly errors are introduced which are reflected in gaps with high stain penetration. It was found however that these irregularities heal out when polysheaths are annealed for extended periods of time. The polysheaths exhibit a similar stability against dissociation as contracted sheath.

Polysheath is identical with contracted sheath except that the latter has a defined length. This length is determined by the length of the core baseplate which serves as a ruler [1]. The length distribution of polysheath is broad and the average length depends on the total P18 concentration and on other polymerization conditions. The determination of size distribution by electronmicroscopy suffers from the inherent uncertainty due to a possible selective adsorption of long particles, breakage of particles by the absorption forces and by other possible artifacts [23]. The evaluation of the size distribution from sedimentation coefficients may be influenced by other systematic errors. Sedimentation coefficients were not extrapolated to zero concentration mainly because the size distribution itself is concentration dependent. Also the relation between length and sedimentation coefficient (eq. (9)) is only approximately valid. In spite of these difficulties it is satisfactory that the size distribution determined by the two methods agree well in the case of polysheath.

The Poisson type size distribution found after spontaneous polymerization is of the type expected for a linear polymerization in which the foreward reaction is much faster than dissociation. [16,18]. It is a so-called kinetically controlled size distribution [18]. The beginning of a redistribution towards an exponential size distribution was observed after several weeks and months. This behaviour is in agreement with theoretical predictions [16,18]. The final exponential equilibrium distribution which is predicted by the equilibrium theory for most association processes [16, 24] is probably established only after extremely long and experimentally unaccessible periods of time.

Acknowledgement

We thank Professor E. Kellenberger for helpful discussions, Ariel Lustig for performing the ultracentrifugal analysis and Dr. Michel Wurtz for his help at the electronmicroscope. This research was supported by the Swiss National Science Foundation through grant no. 3.222.77 and 3.556.0.79.

References

[1] S. Casjens and J. King, Ann. Rev. Biochem. 44 (1975) 555.
[2] L.M. Kozloff and M. Lute, J. Mol. Biol. 234 (1959) 539.
[3] P.R. Smith, U. Aebi, R. Josephs and M. Kessel, J. Mol. Biol. 106 (1976) 243.
[4] L.A. Amos and A. Klug, J. Mol. Biol. 99 (1975) 51.
[5] Y. Kikuchi and J. King, J. Mol. Biol. 99 (1975) 645.
[6] F. Arisaka, J. Tschopp, R. van Driel and J. Engel, J. Mol. Biol. 132 (1979) 369.
[7] M.F. Moody, J. Mol. Biol. 25 (1967) 167.

[8] C.M. To, E. Kellenberger and A. Eisenstark, J. Mol. Biol. 46 (1969) 493.
[9] J. Tschopp, F. Arisaka, R. van Driel and J. Engel, J. Mol. Biol. 128 (1979) 247.
[10] N. Sarkar, S. Sarkar and L.M. Kozloff, Biochemistry 3 (1964) 511.
[11] R.C. Dickson, Virology 59 (1974) 123.
[12] O.H. Lowry, N.J. Rosenbrough, A.L. Farr and R.J. Randall, J. Biol. Chem. 193 (1951) 265.
[13] J.H.K. Schachman, in: Ultracentrifugation in biochemistry (1959) (Academic Press, New York) p. 133.
[14] V.N. Schumaker and H.N. Schachmann, Biochim. Biophys. Acta 23 (1957) 628.
[15] A. Wegner and J. Engel, Biophys. Chem. 3 (1975) 215.
[16] F. Oosowa and S. Asakura, Thermodynamics of the polymerization of protein (Academic Press, New York, 1975).
[17] V. Bloomfield, W.O. Dalton and K.E. van Holde, Biopolymers 5 (1967) 135.
[18] J. Engel and A. Wegner, Studia Biophysica, Berlin 57 (1976) 179.
[19] E. Kellenberger and Boy de la Tour, J. Ultrastr. Res. 11 (1964) 545.
[20] S. Brenner, G. Streisinger, R.W. Horne, S. Champe, L. Barnette, S. Benzer and M.W. Rees, J. Mol. Biol. 1 (1959) 281.
[21] J.A. Luthy, M. Praissman, W.R. Finkenstadt and M. Laskowski Jr., J. Biol. Chem. 248 (1973) 1760.
[22] U. Quast, J. Engel, H. Heumann, G. Krause and E. Steffen, Biochemistry 13 (1974) 2512.
[23] S. Dubochet and E. Kellenberger, Microscopia Acta 72 (1972) 119.